

Long-lasting and responsive DNA/enzyme-based programs in serum-supplemented extracellular media

Jean-Christophe Galas,* André Estevez-Torres,* and Marc Van Der Hofstadt*

1

Sorbonne Université, CNRS, Institut de Biologie Paris-Seine (IBPS), Laboratoire Jean Perrin (LJP), F-75005, Paris, France

E-mail: jean-christophe.galas@upmc.fr; andre.estevez-torres@upmc.fr; marcvdhs@gmail.com

2

Abstract

3

4

5

6

7

8

9

10

11

12

13

14

15

16

17

18

19

DNA molecular programs are emerging as promising pharmaceutical approaches due to their versatility for biomolecular sensing and actuation. However, the implementation of DNA programs has been mainly limited to serum-deprived *in vitro* assays due to the fast deterioration of the DNA reaction networks by the nucleases present in the serum. Here, we show that DNA/enzyme programs are functional in serum for 24h but are latter disrupted by nucleases that give rise to parasitic amplification. To overcome this, we implement 3-letter code networks that suppress autocatalytic parasites while still conserving the functionality of DNA/enzyme programs for at least 3 days in the presence of 10% serum. In addition, we define a new buffer that further increases the biocompatibility and conserves responsiveness to changes in molecular composition across time. Finally, we demonstrate how serum-supplemented extracellular DNA molecular programs remain responsive to molecular inputs in the presence of living cells, having responses 6-fold faster than cellular division rate and are sustainable for at least 3 cellular divisions. This demonstrates the possibility of implementing *in situ* biomolecular characterization tools for serum-demanding *in vitro* models. We foresee that the coupling of chemical reactivity to our DNA programs by aptamers or oligonucleotide conjugations will allow the implementation of extracellular synthetic biology

20 tools, which will offer new biomolecular pharmaceutical approaches and the emergence
21 of complex and autonomous *in vitro* models.

22 **Keywords**

23 DNA molecular programs, Serum, endonuclease, responsive networks, living cells

24 In the last few decades, the programmability and reactivity of DNA has positioned the
25 DNA nanotechnology field as a promising avenue for the development of biomolecular phar-
26 maceutical approaches.¹ In particular, DNA molecular programming tools have been exten-
27 sively used to create bioactuation systems for the delivery of cargoes² and for the modification
28 of cellular composition,³ as well as biosensing tools for cell sorting⁴ and molecular detection.⁵
29 For example, the specific amplification of nucleic acid sequences by polymerase-based DNA
30 programs allows the detection of microRNA biomarkers down to attomolar concentrations
31 with dynamic ranges up to 10 orders of magnitude.⁵ In addition, the amplification of DNA
32 also grants the possibility of implementing DNA molecular computations, which has already
33 been nicely exploited to diagnose cancer profiles from human samples.⁶ However, very few
34 molecular programs work in direct contact with living cells.¹ In contrast, current imple-
35 mentations favour the analysis of liquid biopsies within solutions that are not compatible
36 with cellular growth⁷ or else use compartments that separate the program and the living
37 system.⁸⁻¹⁰ As a result, these approaches limit the implementation of DNA pharmaceutical
38 tools for *in vitro* studies.

39 In an effort to surpass this limitation, we recently demonstrated the embedding of a
40 DNA/enzyme molecular program within the extracellular medium of an *in vitro* cell culture.³
41 Notably, we showed how the programmable extracellular medium was capable of guiding
42 cellular composition across time and space, opening the pathway towards the development
43 of extracellular synthetic biology tools. Nevertheless, the absence of serum reduces the

44 biological significance of that study, since the myriad of bioactive substances provided by
45 the animal serum has become an essential component for successful *in vitro* cell culture.¹¹
46 For this reason, the DNA nanotechnology field has recently focused on the stabilization of
47 DNA nanostructures¹² and DNA circuits within serum-supplemented media.¹³ However, to
48 date, only Fern *et al.* have reported a solution for extending the functional life of DNA-only
49 programs in the presence of serum components.¹⁴ The main limitation emerges from the
50 unwanted interactions of the serum components that alter or degrade the DNA molecules,
51 which leads to the rapid loss of the designed networks. In particular, this low resilience has
52 been mainly attributed to the degradation of the DNA by the presence of nucleases in the
53 serum, which restrains any potential for long-term application of DNA programs.

54 To overcome the degradation of the DNA by the serum, two major approaches have been
55 developed. Firstly, the nuclease activity can be impaired by using DNase inhibitors (such
56 as actin) or by heat inactivating the serum.¹⁵ Secondly, efforts have been focused on the
57 protection of the synthetic DNA strands by the introduction of structural changes, either
58 chemical^{16,17} or morphological.¹⁴ While the first approach is incompatible with nuclease-
59 assisted DNA programs and lacks biological significance (as the heat inactivation denatures
60 all proteins present in the serum), the second is not suitable for polymerase-based DNA
61 programs as the *de novo* synthesized DNA cannot be protected *in situ*. For these reasons, to
62 the best of our knowledge, long-lasting DNA/enzyme molecular programs have not yet been
63 described in the presence of animal serum, limiting the potential of using DNA molecular
64 programs in the presence of living cells for *in situ* biosensing and bioactuation.

65 Here, we demonstrated that a DNA/enzyme-based molecular program is functional in the
66 presence of animal serum and living cells for at least three days. Firstly, we show that the
67 existence of nucleases in the serum disrupt the polymerase-based DNA programs, since the
68 emergence of non-programmed parasitic amplification is enhanced and overtakes the DNA
69 program. To circumvent this, we restrained the undesired activity of serum nucleases by
70 avoiding the creation of *de novo* double stranded DNA (dsDNA) through the use of 3-letter

71 code templates. The reformulated DNA programs were capable of responding to sequence-
72 specific single stranded DNA (ssDNA) and triggering the *in situ* production of ssDNA up
73 to 1 μ M for at least 49 h in the presence of 10% fetal bovine serum. Secondly, we show that
74 such serum conditions are needed to conserve the phenotypic behaviour of *in vitro* human
75 embryonic kidney cells. Finally, we demonstrate that serum-supplemented DNA/enzyme-
76 based extracellular programs remain responsive in the presence of living cells, paving the way
77 for the development of DNA-regulated extracellular synthetic biology systems that would
78 complement traditional intracellular approaches to create complex and autonomous *in vitro*
79 models.

80 Results

81 Serum disrupts the functionality of DNA/enzyme molecular pro- 82 grams

83 To assess the functionality and robustness of DNA/enzyme-based programs in serum, we
84 performed an exponential amplification reaction (EXPAR) in the presence of fetal bovine
85 serum (FBS). In particular, we focused on the polymerase, nickase, exonuclease dynamic
86 network assembly toolbox (PEN DNA toolbox)¹⁸ as it allows the assembly of elementary re-
87 actions (Figure S8) into complex functional reaction networks.^{19,20} Figure 1a exemplifies the
88 behaviour of a PEN DNA autocatalyst, where ssDNA \mathbf{A}_1 is amplified exponentially in the
89 presence of template \mathbf{T}_1 and the three enzymes cited above. The fluorescence of the interca-
90 lator EvaGreen allows to follow, over time, the total concentration of double stranded DNA
91 (dsDNA) in solution. This PEN amplification reaction is characterized by a sigmoidal curve,
92 where an initial exponential phase is followed by a linear phase before reaching saturation.
93 At saturation, the EvaGreen fluorescence reaches a plateau corresponding to a steady state
94 of dsDNA concentration and due to the constant production and degradation of *de novo*
95 DNA by the polymerase and exonuclease, respectively.¹⁸ In a first series of experiments, we

106 tested the autocatalytic template \mathbf{T}_1 in a buffer compatible both with PEN reactions and
107 mammalian cell culture³ (named *Kin* buffer due to its high enzyme kinetics, see SI Section
108 3), for increasing concentrations of serum. In all conditions, we observed a decrease in the
109 fluorescence intensity during the first 500 min (Figure 1b), reduction we account to an arti-
110 fact due to the presence of 0.5x cell culture medium (Dulbecco's modified Eagle's medium,
111 DMEM) in the buffer. However, the onset of the exponential amplification by the autocat-
112 alytic \mathbf{T}_1 template can still be clearly distinguished by the sigmoidal curve starting after
113 500 min in the absence of FBS. Upon the introduction of 2.5% FBS, the DNA amplification
114 dynamics were slowed down (loss in steepness of the linear region) and the dsDNA steady
state regime was not persistent, since it was followed by a nonlinear signal increase after
1800 min. We attribute both these deficiencies to the emergence of untemplated replication
of DNA,²¹ which gives rise to parasitic amplification networks that hijack the enzymes and
energy source. As FBS concentration was further increased, the linear regime shortened and
the nonlinear signal increase started earlier. At 10% FBS (standard cell culture concentra-
tions) the initial exponential amplification regime of the synthetic \mathbf{T}_1 template cannot be
distinguished from the parasitic non-linear amplification. Denaturing polyacrylamide gel
(PAGE) clearly demonstrated the production of copious DNA strands not related to the
original amplification network (SI Section 2), and consequently the loss of the functionality
of the DNA/enzyme molecular program.²²

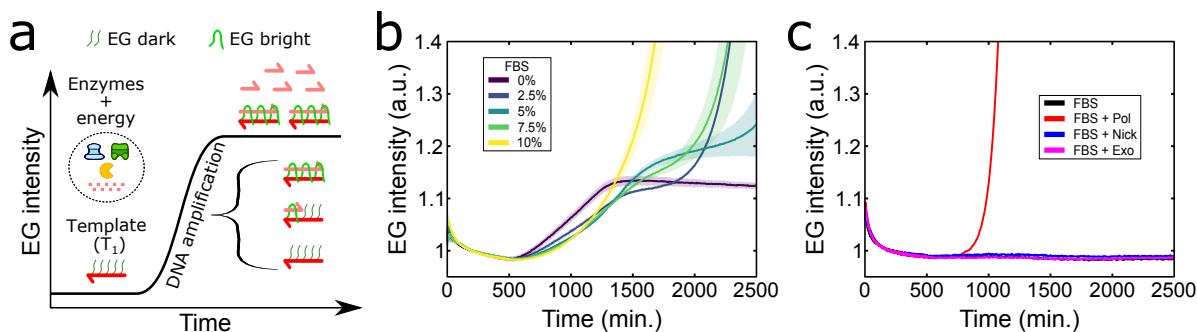


Figure 1: Serum promotes the emergence of parasitic amplification in the presence of polymerase-based DNA programs. (a) Scheme of the PEN DNA exponential amplification reaction depicting the nature and behaviour of the EvaGreen (EG) reporter, a fluorescent dsDNA intercalator, on the autocatalytic T_1 template. Harpoon-ended arrows represent single stranded DNA (ssDNA). (b) EvaGreen fluorescence *versus* time for the T_1 autocatalytic network at 37 °C in a concentration range of FBS. (c) EG fluorescence *versus* time for the incubation of 10% FBS with one of the three enzymes present in PEN reactions: polymerase (pol), Nb.BsmI nickase (nick) or exonuclease (exo). The shades in panel b correspond to one standard deviation of a triplicate experiment. Conditions panel b and c: *Kin* buffer with 0.1 mM dithiothreitol (DTT), in addition to 200 nM of autocatalytic T_1 template for panel b.

115 Although the exact mechanism of parasitic amplification is still not well understood, it
116 is known that it emerges from the *de novo* synthesis of DNA by polymerases²³ and by the
117 presence of endonucleases that create tandem repeats²⁴ and quasi-palindromic sequences,²¹
118 both containing the endonuclease recognition site. For instance, the polymerase and the
119 nicking enzyme of the PEN reactions generate autocatalytic parasites in the presence of
120 dNTPs.²² To test if the observed parasites in the presence of serum (Figure 1b) were due
121 to the PEN nicking enzyme or to an endonuclease present in the serum, we performed
122 the following experiment. In a controlled experiment, we generated a PEN parasite in the
123 presence of Nb.BsmI (the PEN nicking enzyme), and a second with the addition of 10%
124 serum. After parasite had emerged, we incubated both conditions in the presence of BsmI,
125 the corresponding restriction enzyme (SI Section 2). We observed that after 3.5 hours of BsmI
126 incubation, the DNA smear characteristic of PEN parasites observed in denaturing PAGE
127 had been strongly reduced (Figure S1).²¹ In contrast, when we tested the degradability of
128 parasites that had emerged in the presence of 10% FBS, we observed that, after 8 hours of
129 BsmI incubation, the smear had only partially disappeared (Figure S2). We further tested

130 the potential of FBS to give rise *per se* or aided by PEN enzymes to the creation of parasite.
131 We incubated 10% FBS in the absence or in the presence of one of the three enzymes
132 present in PEN reactions and followed EvaGreen fluorescence for exponential amplification
133 of *ab initio* dsDNA (Figure 1c). Results demonstrated that while 10% FBS was not capable
134 of giving rise to parasite autonomously, parasite emerged only when polymerase was added to
135 the FBS solution. In addition, we observed that the parasitic emergence time was inversely
136 proportional to the FBS concentration (Figure S9). We infer that the FBS has endonuclease
137 enzymes that, together with the polymerase and dNTPS used on PEN reactions, generates
138 autocatalytic parasites that disrupts the DNA/enzyme programs.

139 **Impairing serum parasite emergence by using a 3-letter code**

140 We have recently demonstrated that the emergence of PEN parasites can be overcome by
141 selecting a PEN enzyme whose recognition site only bears 3 of the 4 nucleotides per strand,
142 coupled to a 3-letter code template.²² As a result, in the absence of the fourth dNTP in the
143 solution, *de novo* DNA synthesis by the polymerase cannot create *in situ* dsDNA that may be
144 cleaved by the nicking enzyme, thus yielding a parasite (Figure S10).^{21,24} Thus, by designing
145 a PEN autocatalytic network with DNA templates containing only adenine, guanine and
146 cytosine in their sequence, and removing adenosine triphosphate from the dNTPs solution
147 (Figure 2a), one obtains a functional DNA circuit while avoiding the emergence of unwanted
148 parasitic sequences.

149 To investigate if a 3-letter code approach can also impair the emergence of serum-
150 promoted parasites, we first designed an autocatalytic template (\mathbf{T}_2) that was based on
151 the Nb.BssSI nickase, as all thymine bases are located in the same strand of the recognition
152 site, and that worked at 37 °C. Figure 2b shows the amplification dynamics of template \mathbf{T}_2 in
153 the presence of 3 dNTPs and increasing concentrations of serum. The fluorescence intensity
154 displayed a sigmoidal curve characteristic of PEN exponential amplification. Importantly,
155 and contrary to 4-letter code templates (Figure 1b), the amplification dynamics were not

156 significantly affected, for up to 42 h, even in the presence of 10% FBS. We do observe a
157 modest delay on the onset of the exponential amplification upon the addition of 10% FBS
158 associated to a slower nickase kinetics (Figure S3). As expected, parasite emergence was still
159 observed in the presence of 4 dNTPs (Figure S11).

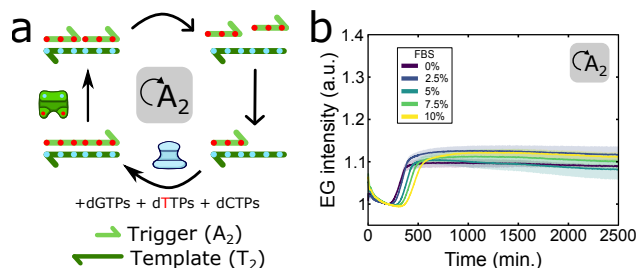


Figure 2: 3-letter code DNA networks preclude the emergence of autocatalytic parasites originating from endonucleases present in the FBS. (a) Scheme of the 3-letter code autocatalyst resistant to parasitic emergence in FBS due to the absence of dATPs in the solution. In this network, the dATPs (blue spots) are restricted to the synthetic T_2 templates and the dTTPs (red spots) to the *de novo* A_2 ssDNA synthesis. Harpoon-ended arrows represent ssDNAs. Irreversible and reversible reactions are indicated by solid and empty arrowheads, respectively. (b) EG fluorescence *versus* time for the T_2 autocatalytic network with the Nb.BssSI nickase at 37 °C in a concentration range of FBS in the absence of dATPs. Note the absence of parasites compared to Figure 1b. The shades in panel b correspond to one standard deviation of a triplicate experiment. Conditions: *Kin* buffer with 0.1 mM DTT.

160 **PEN molecular programs remain responsive for at least 45 h**

161 *In vitro* cellular doubling time largely depends on cellular type and growth conditions, rang-
162 ing from 10 h to few days.²⁵ For example, the doubling time for human cervix epithelial
163 carcinoma cells (HeLa cell line) in our conditions was ~ 17.5 h (Figure S12). In order to
164 develop DNA extracellular programs that may interact with cells, one needs a DNA pro-
165 gram that computes faster than cellular growth (*i.e.* < 15 h) and that remains responsive
166 for at least two cell cycles (*i.e.* > 40 h). To introduce a fast and responsive behaviour into
167 our DNA program, we took advantage of a repression module to implement a controllable
168 bistable switch (Figure 3a).¹⁸ In this network, we define the *ON* state as the result from the
169 sustained exponential amplification of A_2 by the autocatalytic reaction of template T_2 , as
170 it has been shown above. Contrary, in the *OFF* state, the presence of high concentrations of

171 the repressor strand (\mathbf{R}_2) suppresses this autocatalytic reaction due to the combined elimi-
172 nation of \mathbf{A}_2 by the exonuclease and its conversion to waste (\mathbf{W}) by \mathbf{R}_2 . However, the *OFF*
173 state can be reverted to the *ON* state by the addition of a DNA activator (\mathbf{R}_2^*), comple-
174 mentary to \mathbf{R}_2 , that reactivates the exponential amplification of \mathbf{A}_2 .³ The program is thus
175 *responsive* to the molecular stimulus of \mathbf{R}_2 . Note that, due to the low dNTPs consumption
176 rate of the system in the *OFF* state, we expect the DNA program to remain responsive for
177 long periods of time.

178 To determine if the DNA program remained responsive in the presence of 10% FBS, we
179 spiked the *OFF* state with 200 nM of \mathbf{R}_2^* at different time points (Figure 3b and Figure S6).
180 Since the dithiothreitol (DTT) prevents the oxidation of the enzymes,²⁶ we hypothesized
181 that increasing its concentration could help keeping the amplification onset time (τ) and the
182 fluorescent amplitude of the response (ΔI) constant at longer times. We observed that the
183 responsive time for up to 1868 min changed little for DTT concentrations ranging 0.2-0.5
184 mM (Figure 3c). In contrast, at 2700 min, increasing DTT concentration from 0.2 up to 0.5
185 mM made the response 26 % faster. Nevertheless, in all cases, the system was capable of
186 responding at least 4.6-fold faster than HeLa cellular division rate and for at least 2.5 cell
187 cycles.

188 The amplitude of the response (the steady-state signal of the fluorescently-labeled tem-
189 plate, see SI Section 3) is also important for bioactuation purposes. Since we noticed that
190 the ΔI at twice the onset time (2τ) was decreasing with the injection time (Figure 3b and
191 Figure S13), we evaluated the DNA concentration behaviour across time. To do so, we
192 quantified the \mathbf{A}_2 ssDNA available after a 49 h run for an experiment spiked at 0, 24 and
193 40 h (Figure S14). When spiked at $t = 0$ h, the DNA program produced respectively 0.8
194 μM and 1.1 μM of \mathbf{A}_2 in the presence of 0.2 and 0.5 mM DTT, which is ~ 5 -fold greater
195 than the template concentration (Figure 3d). We observed that these levels were similarly
196 reached for experiments spiked after 24 h. Regarding 40 h spiked experiments, the produc-
197 tion of \mathbf{A}_2 could only reach $53 \pm 1\%$ when 0.2 mM DTT was used. However, this production

198 increased up to $89 \pm 15\%$ in the presence of 0.5 mM DTT, showing the great robustness
 199 of PEN networks in the presence of serum. Furthermore, since the onset of the exponential
 200 amplification is dependent on \mathbf{R}_2^* concentration (Figure S15), the designed DNA program
 201 will also be capable of quantifying changes in molecular composition.

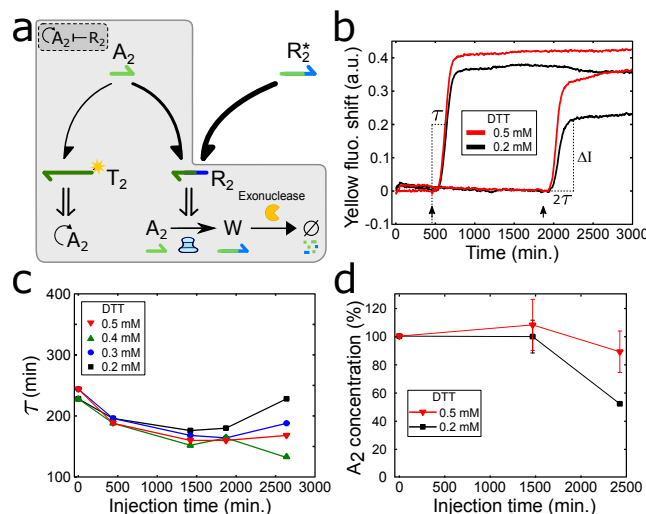


Figure 3: Long-lasting and responsive DNA programs in the presence of 10% FBS. (a) Scheme of the responsive DNA program. The combination of an autocatalytic node (\mathbf{T}_2) with a repressor node (\mathbf{R}_2) allows the creation of a bistable switch (grey enclosure), where the higher affinity of \mathbf{A}_2 with \mathbf{R}_2 compared with \mathbf{T}_2 causes the extension of \mathbf{A}_2 to a non functional ssDNA (waste \mathbf{W}) and its degradation by the exonuclease. The addition of \mathbf{R}_2^* that binds to \mathbf{R}_2 reduces the free concentration of the latter, promoting the exponential amplification of \mathbf{A}_2 by \mathbf{T}_2 . The thickness of half arrow-headed lines indicates DNA affinities. (b) Fluorescence shift from the fluorescently-labeled \mathbf{T}_2 versus time for the responsive program triggered at different times with \mathbf{R}_2^* and for different [DTT] on the *Kin* buffer. The amplification onset time, τ , and the fluorescent amplitude of the response at dsDNA steady state, ΔI , are defined on the graph (see methods). (c) τ versus the time at which \mathbf{R}_2^* was introduced into the solution (injection time) at different [DTT]. (d) \mathbf{A}_2 relative concentrations at steady state with respect to the value obtained for an injection time at $t = 0$ h, for different injection times and [DTT] (Figure S14). Data in panel c determined from panel b and Figure S6. Solid lines in panel c and d are guides to the eye. Error bars in panel d correspond to the standard deviation of a triplicate experiment. Conditions: $[\mathbf{R}_2]_0 = 100$ nM. 200 nM of \mathbf{R}_2^* was added at the injection times (arrowheads in panel b).

202 Increasing the biocompatibility of the buffer

203 We have demonstrated that greater DTT concentrations improve the responsiveness of the
 204 DNA program in the presence of serum. However, since high levels of [DTT] decrease cell

205 viability, as they transiently activate endoplasmic reticulum stress²⁷ and cause cell detach-
206 ment,³ we decided to further increase the biocompatibility of our buffer to mitigate cyto-
207 toxicity (although the introduction of FBS already partially attenuates the adverse effect
208 of DTT, Figure S16). To do so, we increased the concentration of the cell culture medium
209 (from 0.5x to 0.89x), we removed non-critical PEN buffer components and lowered the con-
210 centration of magnesium (SI Section 3) to create a new buffer that we named *Cell+* buffer.
211 Interestingly, we observed that the chosen 3-letter code nickase (Nb.BssSI) was more robust
212 to buffer modifications than the traditional Nb.BsmI nickase used for PEN reactions and
213 that they were also functional in RPMI-1640, another standard cell culture media (Figure
214 S7).

215 In contrast with the results shown above in the *Kin* buffer, we observed that the τ and
216 \mathbf{A}_2 concentrations at steady state in the *Cell+* buffer were strongly dependent on [DTT]
217 and injection time (Figure 4 and Figure S13). In particular, we observed that at low DTT
218 concentrations (0.2 mM) τ values increased by 139% when the DNA program was activated
219 after 45 h. However, at higher concentrations (>0.3 mM) the DTT concentration had no
220 further effect. Quantification of the available \mathbf{A}_2 at steady state revealed that it decreased
221 steadily at longer injection times. When the injection occurred at 24 h, \mathbf{A}_2 was produced at
222 $\sim 75\%$ of the steady state level when injected at $t = 0$ h. Regarding the injection at 40 h,
223 \mathbf{A}_2 dropped to $26 \pm 5\%$ and $60 \pm 6\%$ for the 0.2 and 0.3 mM of DTT, respectively. As the
224 response (τ and $[\mathbf{A}_2]$) is not largely affected when the [DTT] is increased above 0.3 mM, we
225 decided to use this concentration of DTT to have a compromise between functionality and
226 biocompatibility for the new *Cell+* buffer.

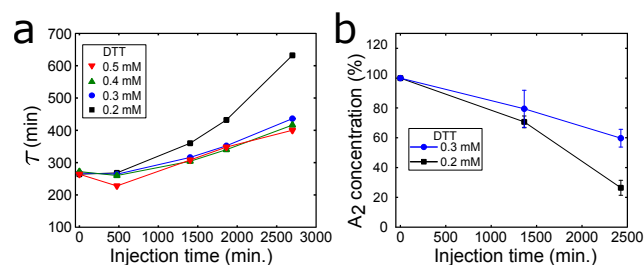


Figure 4: Responsiveness of the DNA program in the *Cell+* buffer. (a) τ versus injection time of \mathbf{R}_2^* in *Cell+* buffer in a range of [DTT]. (b) A_2 concentration for the injection of \mathbf{R}_2^* after 24 h and 40 h quantified from Figure S14. Data in panel a determined from Figure S6. Solid lines are guides to the eye. Error bars in panel b correspond to the standard deviation of a triplicate experiment. Conditions: $[\mathbf{R}_2]_0 = 100$ nM. 200 nM of \mathbf{R}_2^* was added at the injection times.

227 Once that we have evaluated the performances of the DNA/enzyme program in the serum-
228 supplemented *Kin* and *Cell+* buffers, it is now necessary to measure cellular viability in these
229 buffers. To do so, HeLa cells were stained with propidium iodide and their fluorescence
230 evaluated using flow cytometry at different culture times (Figure 5a and Figure S12). As
231 expected, in the control condition the number of living cells increased with time. However,
232 we noticed a 1.6-fold reduction on cellular growth rate after 48h that didn't occur in the
233 absence of FBS (Figure S12), most likely indicating an impairment on cell growth due to the
234 exposition to serum-supplemented media for long periods of time (e.g. high metabolism). To
235 test the biocompatibility of the *Kin* buffer, we decided to use 0.5 mM DTT to conserve the
236 fast and long-lasting responsiveness of the DNA program assessed in the previous section.
237 Results revealed a significant reduction on cellular viability (down to 71%) and 3.6-fold
238 lower cell number after 24h compared to the control, which we attribute to the toxicity and
239 cellular detachment introduced by the high DTT concentration. On the other hand, the
240 *Cell+* buffer at 0.3 mM DTT conserved high viability (above 93%) and similar cell number
241 after 24h of incubation as the control. Although we found an average ~ 2 -fold reduction in
242 growth rate compared to the control, a ~ 2 -fold increase in viable cell number after 48 h was
243 achieved compared to previously reported experimental conditions in the absence of FBS
244 (*Kin* buffer).³

245 To stress the importance of developing serum-compatible DNA/enzyme programs, we
246 studied the growth of human embryonic kidney 293 cells (HEK 293 cell line), as their be-
247 haviour (e.g. signalling pathways) is significantly affected by serum starvation.²⁸ We ob-
248 served that in the absence of serum, HEK cells aggregated in standard cell culture medium,
249 phenotype that was not appreciable when supplemented with 10% FBS (Figure 5b). We
250 noted that the stretched morphology was still conserved for at least 48 h when the FBS was
251 reduced down to 2.5% (Figure S17), opening the possibility to reduce the FBS concentration
252 without perturbing cellular phenotype. When we evaluated the morphology and viability of
253 HEK cells in the two DNA buffers, we noticed that, contrary to HeLa cells, HEK cells are
254 less resilient to the presence of DTT (Figure S18), most likely due to their lower adhesion to
255 surfaces. Nevertheless, HEK cells conserved high cellular viability and stretched morphology
256 in the serum-supplemented *Cell+* buffer in contrast to what happened in the *Kin* buffer
257 (Figure 5b and Figure S12).

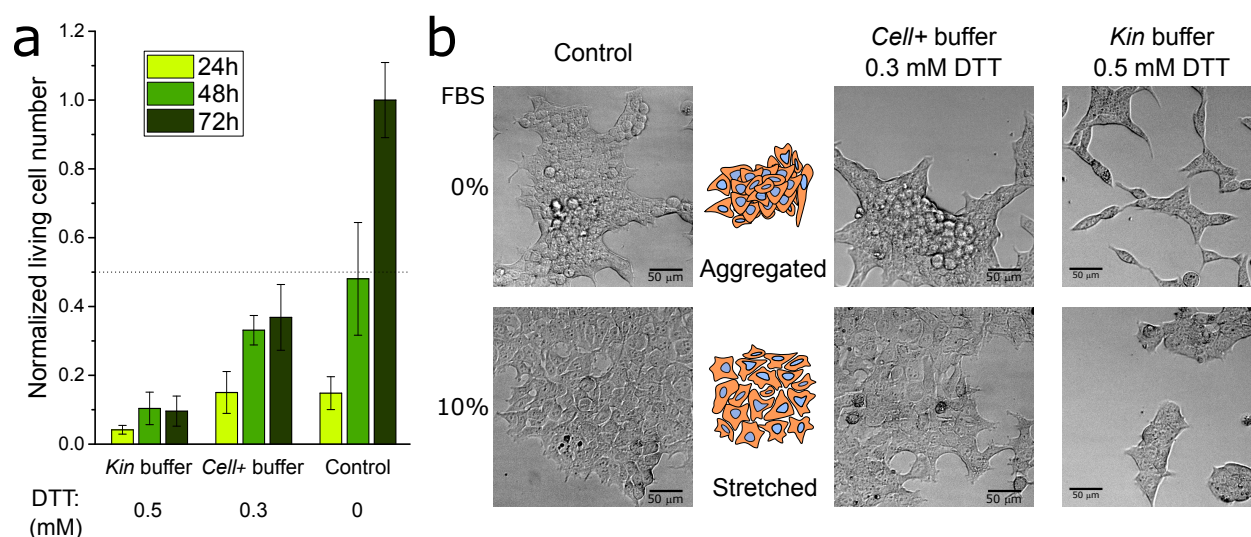


Figure 5: Evaluation of cell viability for the three buffers used in this study. (a) Normalized living cell number of HeLa cells determined by cellular staining with propidium iodide and flow cytometry for different incubation times and conditions in the presence of 10% FBS. Data determined from Figure S12. (b) Bright-field images demonstrating the morphology of HEK cells after 72 h of incubation in the absence or the presence of 10% FBS for the control growth medium, *Cell+* buffer and *Kin* buffer. Images obtained from the time-lapse of Figure S19.

258 Serum-supplemented DNA programs are functional in the presence 259 of cells

260 To verify that the DNA/enzyme program was still functional in the presence of living cells
261 and 10% FBS, we first tested the bistable switch. To do so, we seeded the cells in a cell
262 culture multiwell plate, and allowed them to adhere for 24 h before introducing the *Cell+*
263 buffer containing the DNA program (Figure 6a). When the DNA program was set to be in
264 the *ON* state ($[\mathbf{R}_2]_0 = 0$ nM), the exponential amplification of DNA occurred within 2 h and
265 reached a steady state after 23 h (Figure 6b). When the program started in the *OFF* state
266 ($[\mathbf{R}_2]_0 = 150$ nM), the amplification of DNA was suppressed for at least 71 h, showing the
267 robustness of the *OFF* state in the presence of living cells. Quantification of the available
268 \mathbf{A}_2 at steady state revealed that the same concentration of ssDNA was produced for the *ON*
269 state in the absence (Figure 3d) and in the presence of cells (Figure 6c), and that no \mathbf{A}_2 was
270 produced in the *OFF* state.

271 To test the responsiveness of the DNA program in the presence of living cells, the *OFF*
272 state was turned *ON* by the addition of 300 nM of \mathbf{R}_2^* after 24 h or 40 h. In both cases,
273 we observed that the amplification of DNA was initiated within 3 h, which is ~ 6 -fold faster
274 than cellular growth rate, and reached a steady state after ~ 15 h, where it remained until
275 the end of the experiment. However, we noticed a $\sim 50\%$ reduction in the dsDNA steady-
276 state fluorescence compared to the *ON* state. The quantification of \mathbf{A}_2 showed that the
277 injections at 24 and 40 h produced 210 and 134 nM of \mathbf{A}_2 , respectively. This is 2-3 times
278 less than what was produced in the *ON* state but still remarkable and largely sufficient to
279 perform downstream molecular computations. We hypothesize that this reduction is due
280 to the presence of cells, either due to the cell debris and secretions that may interfere with
281 the DNA/enzyme program, or due to a greater DNA uptake by cells due to the presence of
282 FBS.²⁹ In addition, we contemplate that in early activated DNA programs, due to the high
283 concentration of *de novo* \mathbf{A}_2 ssDNA compared to the initial synthetic template \mathbf{T}_2 , the core
284 of the DNA program (*i.e.* the template) is significantly less affected by the presence of cells.

285 Similar results were obtained for the lesser biocompatible *Kin* buffer, although with a faster
 286 response and higher A_2 concentrations at steady state (Figures S20 and S21). Finally, clock
 287 reactions controlling the onset time of the exponential amplification in a pre-encoded manner
 288 were also functional in the presence of serum (Figure S21). These results demonstrate the
 289 feasibility of programmable and responsive DNA/enzyme based molecular programs in the
 290 presence of cells and 10% serum.

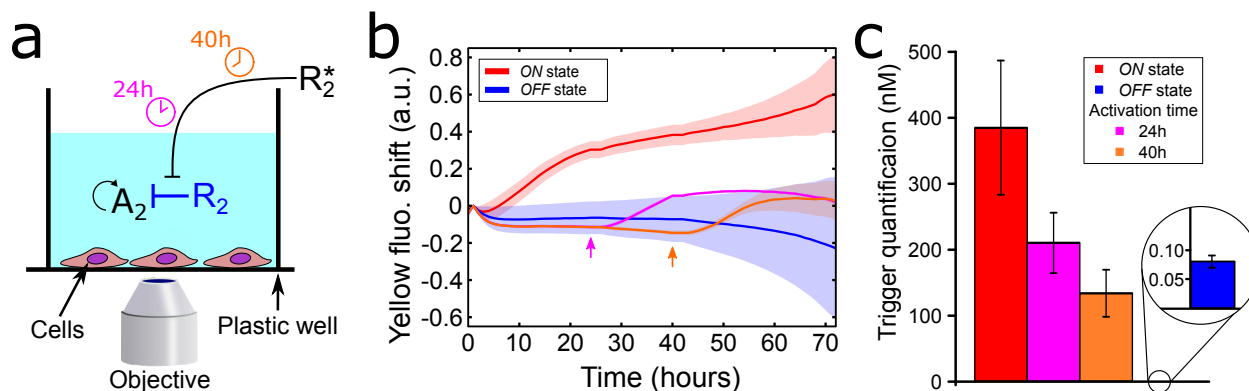


Figure 6: Long-lasting and responsive behaviours of serum-supplemented extracellular DNA programs in the presence of living cells. (a) Cartoon of the experimental setup (not to scale). The cells are cultured in the extracellular DNA program where the A_2 autocatalyst is not suppressed (*ON* state) or permanently repressed (*OFF* state). In the later case, the *OFF* state can be reverted by the external addition of DNA activator R_2^* after 24 h (pink) or 40 h (orange). (b) Fluorescence shift of T_2 versus time showing the production dynamics of A_2 in the *Cell+* buffer in the presence of 10% FBS and HeLa cells. The curves show the unsuppressed *ON* state (red) and the repressed *OFF* state (blue) and its responsiveness by the addition of R_2^* at 24 h (pink) and 40 h (orange). Arrowheads indicate the addition time of DNA activator R_2^* . (c) A_2 trigger concentrations after 71h of incubation of the DNA/enzyme-based molecular program in the presence of cells and 10% FBS. Data in panel c determined from Figure S20. Conditions: The *ON* and *OFF* states started with $[R_2]_0 = 0$ nM and 150 nM, respectively. The DNA activator R_2^* was introduced at 300 nM.

291 Conclusions

292 In this paper, we demonstrate the co-existence of responsive DNA/enzyme-based programs
 293 and living cells in the presence of 10% animal serum for at least 3 days, opening a route to
 294 the implementation of *in situ* molecular characterization tools. We have shown that the long-
 295 lasting programmability of polymerase-based DNA programs in the presence of serum is lost

in under one day due to the unwanted nuclease activity present in FBS, which gives rise to parasitic amplification that hijack the enzymes and energy source of the PEN DNA reaction networks. To overcome the emergence of parasites, we used DNA circuits that have been designed to only have 3 deoxynucleotides per strand instead of the traditional 4-letter code. By removing autocatalytic parasites, we could generate a DNA/enzyme program that was responsive for >45h in serum-supplemented buffers. Results revealed that the responsive behaviour to the activation of a bistable DNA switch was capable of producing and maintaining *in situ* up to 1 μ M of ssDNA for at least 49 h. In addition, cellular viability results revealed a \sim 2-fold increase in viable cell number of our serum-supplemented DNA programs in the new *Cell+* buffer in comparison to previous conditions in the absence of FBS.³ Importantly, we have demonstrated that serum-supplemented buffers are capable of conserving the normal stretched phenotype of HEK cells, stressing the importance of developing serum-compatible molecular programs when adventuring for *in vitro* cell culture experiments. Finally, our cell culture results corroborate that serum-supplemented extracellular DNA molecular programs in the presence of living cells are functional, are pre-programmable, can respond to extracellular perturbations faster than cellular division rates and are sustainable for at least 3 cellular divisions (71 h).

The DNA network and buffer optimization shown here can be further extended to other DNA programs and other cell types with adequate modifications. For instance, due to the lower abundance of 3-letter code nucleases,³⁰ we hypothesize that the implementation of DNA-only networks based on 3 deoxynucleotides per strand can reduce the presence of restriction sites of serum nucleases that passively degrade the DNA circuits.¹⁴ Regarding other cell types, we have shown that the DNA program is capable of working in two of the most standard cell culture media (DMEM and RPMI-1640), opening the possibility of its implementation to other cell types with sufficient adaptation. In particular, we stress the fact that we have shown functionality of the DNA program under the conventional use of 10% FBS for cell culture, but not all cells require 10% FBS to conserve growth and phenotype.

323 This grants the opportunity for reducing the concentration of FBS in the presence of the
324 DNA program, which would imply the lower need of [DTT] for DNA responsiveness and
325 hence the buffer would present even lower cytotoxicity for sensitive cell types (*e.g.* neurons).

326 With these outcomes, we now envision the implementation of extracellular DNA pro-
327 grams capable of responding to changes in the molecular composition in the presence of
328 living cells. In particular, the extracellular DNA programs will allow the *in situ* biomolec-
329 ular recognition during *in vitro* cell culture, avoiding *ex situ* non-biocompatible amplifica-
330 tion mechanisms that lack temporal and spatial resolution.⁵ Furthermore, since the PEN
331 DNA toolbox offers a large set of functional reaction networks, such as biochemical concen-
332 tration patterns^{20,31,32} and trigger-driven networks^{33,34} with out-of-equilibrium properties,
333 DNA molecular programs have potential to be advantageously used to create extracellular
334 synthetic biology approaches. These approaches can be coupled to the abundant array of
335 reactivity offered by oligonucleotides, either chemical³⁵ or structural,³⁶ to offer new biomolec-
336 ular pharmaceutical tools. Likewise, communication pathways from the cells to the synthetic
337 programs may be implemented by means of natural precursors (digestion, internalization)
338 or synthetic approaches relying on biomolecular triggers,³⁷ which could be merged to the
339 reactivity of oligonucleotides for the creation of complex and autonomous *in vitro* models.

340 Methods

341 The design of all DNA strands (Table S2) was done heuristically and assisted by Nupack,³⁸
342 and purchased from Integrated DNA Technologies, Inc (U.S.) or Biomers (Germany). Both
343 nickases (Nb.BssSI and Nb.BsmI) and the Bst DNA polymerase large fragment were pur-
344 chased from New England Biolabs. The *Thermus thermophilus* RecJ exonuclease was pro-
345 duced in the lab following previous protocols.³⁹ Standard enzymatic concentrations used
346 in this study were 8 U/mL polymerase, 100 U/mL Nb.BsmI and 31.25 nM exonuclease for
347 Nb.BsmI experiments, and 6.4 U/mL polymerase, 20 U/mL Nb.BssSI and 50 nM exonuclease

348 for Nb.BssSI experiments.

349 The cell growth medium contained Dulbecco's modified Eagle's medium (DMEM F12,
350 PAN Biotech P04-41150) supplemented with 1% Penicillin-Streptomycin. While *Kin* buffer
351 was the previously developed biocompatible medium,³ *Cell+* buffer was a further optimiza-
352 tion to reduce toxicity without drastically losing DNA programmability (SI Section 3). Only
353 *Kin* buffer and *Cell+* buffer contained dXTPs (where *X* could be 3 or N, see Table S1) at
354 0.8 mM. Unless otherwise mentioned, all experiments were performed at 37 °C and 200 nM
355 DNA Template. DNA sequences, buffer composition and further experimental procedures
356 can be found in the Supplementary Information.

357 **PEN reactions in the absence of cells**

358 Experiments were done in 20 μ L solutions and the dynamics of the PEN reactions were
359 exposed by fluorescent changes recorded by a Qiagen Rotor-Gene qPCR machine or a CFX96
360 Touch Real-Time PCR Detection System (Bio-Rad). EvaGreen was used at 0.5x to detect
361 parasite emergence. To remove artifacts due to the perturbation of the solution when the
362 DNA activator \mathbf{R}_2^* was introduced and the opening of the thermal cycler machine, a home
363 made Matlab (The Mathworks) script was used to mathematically equal the fluorescence
364 before and after the perturbation. To calculate the fluorescence shift, the raw fluorescence
365 intensity was corrected by an early time point and subtracted from 1, as done previously.²⁰
366 Both procedures are detailed in SI Section 1.2. For EvaGreen intensity values, the raw
367 fluorescence intensity was only corrected by an early time point. To calculate the onset
368 amplification time, τ , the sigmoidal curve was fitted with a polynomial fit, followed by the
369 derivative of the polynomial fit. The time point with the highest derivative value was chosen
370 as the τ value. The amplitude of the response (ΔI) was measured at the time point when
371 the exponential amplification reached dsDNA steady state. We defined this ΔI time point as
372 the time point when twice the onset amplification time from the perturbation of the system
373 has been attained.

374 **Cell culture handling and experiments**

375 Human cervix epitheloid carcinoma cells (HeLa cell line) and Human embryonic kidney 293
376 cells (HEK 293 cell line) were grown at 37 °C and 5% CO₂. To reduce the cellular shock upon
377 removal of FBS, the cells were grown in two sequential steps of FBS (Dominique Dutscher:
378 S1810-500) (10% and 5%) before maintaining cell culture growth at 2.5% FBS. Bright-
379 field images for observing cellular morphology were obtained with a Zeiss Axio Observer Z1
380 microscope with a 10X objective. When cells reached 80-90% confluence, they were detached
381 with trypsin-EDTA (PAN Biotech: P10-019100) and diluted into fresh 2.5% FBS cell growth
382 medium. For experiments, 800 cells were seeded in 384 cell well plates (ThermoFisher:
383 142762) and allowed to adhere onto the surface for 24 h before replacing the medium with
384 50 μL of the experimental condition.

385 To quantify cellular viability by fluorescenceactivated cell sorting (FACS), the experi-
386 mental condition was replaced with 50 μL trypsin-EDTA (stock solution) and incubated for
387 8 minutes prior inactivation with 50 μL of 10% FBS-supplemented cell growth medium. The
388 cell suspension was mixed with 150 μL FACSFlow (Fisherscientific: 12756528) and 0.5 μL
389 of propidium iodide (~15 mM, ThermoFisher: P3566). The propidium iodide was excited
390 with a 488 nm argon ion laser equipped within the Becton-Dickinson flow cytometer (FAC-
391 SCalibur), and the fluorescent emission recorded within the fluorescence channel FL-2 (band
392 pass 585/42 nm). Cells were quantified for 3 min at a flow of 60 μL/min, and data was
393 treated and analysed with a home-made Matlab routine. Cell count number was divided by
394 the control growth medium to obtain the normalized living cell number.

395 **PEN reactions in the presence of cells**

396 Cells and PEN reactions were monitored using a fully automated Zeiss Axio Observer Z1
397 epifluorescence microscope equipped with a ZEISS Colibri 7 LED light, YFP filter set, and a
398 Hamamatsu ORCA-Flash4.0V3 inside a Zeiss incubation system to regulate temperature at
399 37 °C, in the presence of high humidity and at 5% CO₂. Fluorescence images were recorded

400 every 1 h with a 2.5X objective.

401 Images and data were treated as previously reported.³ Briefly, an ImageJ / Fiji (NIH)
402 routine was implemented to stack the time-lapse images of each well. Subsequently, a Matlab
403 routine was used to create an intensity profile across time of each well, which was divided by
404 an initial time point to correct from inhomogeneous illumination between wells. To correct
405 for time-dependent artifacts (e.g evaporation), the profiles were normalized with a negative
406 control (absence of enzymes, $n = 2$). Lastly, fluorescent jumps and fluorescence shifts were
407 calculated as described above.

408 Available A_2 ssDNA quantification

409 Samples were extracted from the condition of interest and diluted down to 0.025% or 0.075%
410 into a fresh isothermal amplification reaction containing $[T_2]_0 = 50$ nM. The amplification
411 onset times (τ) were plotted within a trigger titration calibration curve for extrapolating
412 the quantification of the available A_2 ssDNA. To avoid perturbations from the FBS or the
413 buffer sample, the fresh isothermal was performed with standard PEN DNA toolbox buffer
414 that contains 3 mM DTT.²⁰

415 Supporting information

416 The Supporting Information contains further experimental methodology, a discussion on
417 parasitic emergence by FBS and details on the buffers, DNA sequences, 23 supporting figures.

418 Acknowledgements

419 We thank Stéphanie Bonneau and Ramón Eritja for supplying the HeLa cells, and Matthieu
420 Morel the HEK 293 cells, Yannick Rondelez and Guillaume Ginés for insightful discussions,
421 and Nelly Henry for the assistance with the FACS. We also thank the financial support from

422 the European Research Council (ERC) under the European's Union Horizon 2020 program
423 (grant no. 770940, A.E.-T.), by the Ville de Paris Emergences program (Morphoart, A.E.-
424 T.), by a Marie Skłodowska-Curie fellowship (grant no. 795580, M.vdH.) from the European
425 Union's Horizon 2020 program, and by a PRESTIGE grant (grant no. 609102, M.vdH.) from
426 the European Union's Seventh Framework Programme.

427 References

- 428 (1) Chen, Y.-J.; Groves, B.; Muscat, R. A.; Seelig, G. DNA nanotechnology from the test
429 tube to the cell. *Nature Nanotechnology* **2015**, *10*, 748–760.
- 430 (2) Li, S. et al. A DNA nanorobot functions as a cancer therapeutic in response to a
431 molecular trigger in vivo. *Nature Biotechnology* **2018**, *36*, 258–264.
- 432 (3) Van Der Hofstadt, M.; Galas, J.-C.; Estevez-Torres, A. Spatiotemporal Patterning of
433 Living Cells with Extracellular DNA Programs. *ACS Nano* **2021**, *15*, 1741–1752.
- 434 (4) Song, T.; Shah, S.; Bui, H.; Garg, S.; Eshra, A.; Fu, D.; Yang, M.; Mokhtar, R.; Reif, J.
435 Programming DNA-Based Biomolecular Reaction Networks on Cancer Cell Membranes.
436 *Journal of the American Chemical Society* **2019**, *141*, 16539–16543.
- 437 (5) Gines, G.; Menezes, R.; Xiao, W.; Rondelez, Y.; Taly, V. Emerging isothermal amplifi-
438 cation technologies for microRNA biosensing: Applications to liquid biopsies. *Molecular*
439 *Aspects of Medicine* **2020**, *72*, 100832.
- 440 (6) Zhang, C.; Zhao, Y.; Xu, X.; Xu, R.; Li, H.; Teng, X.; Du, Y.; Miao, Y.; Lin, H.-c.;
441 Han, D. Cancer diagnosis with DNA molecular computation. *Nature Nanotechnology*
442 **2020**,
- 443 (7) Gines, G.; Menezes, R.; Nara, K.; Kirstetter, A.-S.; Taly, V.; Rondelez, Y. Isother-

- 444 mal digital detection of microRNAs using background-free molecular circuit. *Science*
445 *Advances* **2020**, *6*, eaay5952.
- 446 (8) Chen, J.; Yin, W.; Ma, Y.; Yang, H.; Zhang, Y.; Xu, M.; Zheng, X.; Dai, Z.; Zou, X.
447 Imaging of intracellular-specific microRNA in tumor cells by symmetric exponential
448 amplification-assisted fluorescence in situ hybridization. *Chemical Communications*
449 **2018**, *54*, 13981–13984.
- 450 (9) Joesaar, A.; Yang, S.; Bögels, B.; van der Linden, A.; Pieters, P.; Kumar, B. V. V. S. P.;
451 Dalchau, N.; Phillips, A.; Mann, S.; de Greef, T. F. A. DNA-based communication in
452 populations of synthetic protocells. *Nature Nanotechnology* **2019**, *14*, 369–378.
- 453 (10) Toparlak, D.; Zasso, J.; Bridi, S.; Serra, M. D.; MacChi, P.; Conti, L.; Baudet, M. L.;
454 Mansy, S. S. Artificial cells drive neural differentiation. *Science Advances* **2020**, *6*,
455 eabb4920.
- 456 (11) Brunner, D. Serum-free cell culture: the serum-free media interactive online database.
457 *ALTEX* **2010**, *27*, 53–62.
- 458 (12) Chandrasekaran, A. R. Nuclease resistance of DNA nanostructures. *Nature Reviews*
459 *Chemistry* **2021**, *5*, 225–239.
- 460 (13) Jeong, D.; Klocke, M.; Agarwal, S.; Kim, J.; Choi, S.; Franco, E.; Kim, J. Cell-Free
461 Synthetic Biology Platform for Engineering Synthetic Biological Circuits and Systems.
462 *Methods and Protocols* **2019**, *2*, 39.
- 463 (14) Fern, J.; Schulman, R. Design and Characterization of DNA Strand-Displacement Cir-
464 cuits in Serum-Supplemented Cell Medium. *ACS Synthetic Biology* **2017**, *6*, 1774–1783.
- 465 (15) Hahn, J.; Wickham, S. F. J.; Shih, W. M.; Perrault, S. D. Addressing the Instability of
466 DNA Nanostructures in Tissue Culture. *ACS Nano* **2014**, *8*, 8765–8775.

- 467 (16) Liu, Q.; Liu, G.; Wang, T.; Fu, J.; Li, R.; Song, L.; Wang, Z.-G.; Ding, B.; Chen, F.
468 Enhanced Stability of DNA Nanostructures by Incorporation of Unnatural Base Pairs.
469 *ChemPhysChem* **2017**, *18*, 2977–2980.
- 470 (17) Mallette, T. L.; Stojanovic, M. N.; Stefanovic, D.; Lakin, M. R. Robust Heterochiral
471 Strand Displacement Using Leakless Translators. *ACS Synthetic Biology* **2020**, *9*, 1907–
472 1910.
- 473 (18) Montagne, K.; Gines, G.; Fujii, T.; Rondelez, Y. Boosting functionality of synthetic
474 DNA circuits with tailored deactivation. *Nature Communications* **2016**, *7*, 13474.
- 475 (19) Montagne, K.; Plasson, R.; Sakai, Y.; Fujii, T.; Rondelez, Y. Programming an in vitro
476 DNA oscillator using a molecular networking strategy. *Molecular Systems Biology* **2011**,
477 *7*, 466.
- 478 (20) Zadorin, A. S.; Rondelez, Y.; Gines, G.; Dilhas, V.; Urtel, G.; Zambrano, A.;
479 Galas, J. C.; Estevez-Torres, A. Synthesis and materialization of a reaction-diffusion
480 French flag pattern. *Nature Chemistry* **2017**, *9*, 990–996.
- 481 (21) Tan, E.; Erwin, B.; Dames, S.; Ferguson, T.; Buechel, M.; Irvine, B.; Voelkerding, K.;
482 Niemz, A. Specific versus nonspecific isothermal DNA amplification through ther-
483 mophilic polymerase and nicking enzyme activities. *Biochemistry* **2008**, *47*, 9987–9999.
- 484 (22) Urtel, G.; Van Der Hofstadt, M.; Galas, J.-C. J. C.; Estevez-Torres, A. REXPAR: An
485 Isothermal Amplification Scheme That Is Robust to Autocatalytic Parasites. *Biochem-*
486 *istry* **2019**, *58*, 2675–2681.
- 487 (23) Schachman, H.; Adler, J.; Radding, C. M.; Lehman, I.; Kornberg, A. Enzymatic Syn-
488 thesis of Deoxyribonucleic Acid. *Journal of Biological Chemistry* **1960**, *235*, 3242–3249.
- 489 (24) Zyrina, N. V.; Zheleznaya, L. A.; Dvoretzky, E. V.; Vasiliev, V. D.; Chernov, A.;
490 Matvienko, N. I. N.BspD6I DNA nickase strongly stimulates template-independent syn-

- thesis of non-palindromic repetitive DNA by Bst DNA polymerase. *Biological Chemistry* **2007**, *388*, 367–372.
- (25) Assanga, I. Cell growth curves for different cell lines and their relationship with biological activities. *International Journal of Biotechnology and Molecular Biology Research* **2013**, *4*, 60–70.
- (26) Baccouche, A.; Montagne, K.; Padirac, A.; Fujii, T.; Rondelez, Y. Dynamic DNA-toolbox reaction circuits: A walkthrough. *Methods* **2014**, *67*, 234–249.
- (27) XIANG, X.-Y.; YANG, X.-C.; SU, J.; KANG, J.-S.; WU, Y.; XUE, Y.-N.; DONG, Y.-T.; SUN, L.-K. Inhibition of autophagic flux by ROS promotes apoptosis during DTT-induced ER/oxidative stress in HeLa cells. *Oncology Reports* **2016**, *35*, 3471–3479.
- (28) Pirkmajer, S.; Chibalin, A. V. Serum starvation: caveat emptor. *American Journal of Physiology-Cell Physiology* **2011**, *301*, C272–C279.
- (29) Geary, R. S.; Norris, D.; Yu, R.; Bennett, C. F. Pharmacokinetics, biodistribution and cell uptake of antisense oligonucleotides. *Advanced Drug Delivery Reviews* **2015**, *87*, 46–51.
- (30) REBASE Enzymes, <http://rebase.neb.com/rebase/rebase.enz.html>.
- (31) Zadorin, A. S.; Rondelez, Y.; Galas, J.-C.; Estevez-Torres, A. Synthesis of Programmable Reaction-Diffusion Fronts Using DNA Catalyzers. *Physical Review Letters* **2015**, *114*, 068301.
- (32) Padirac, A.; Fujii, T.; Estévez-Torres, A.; Rondelez, Y. Spatial Waves in Synthetic Biochemical Networks. *Journal of the American Chemical Society* **2013**, *135*, 14586–14592.
- (33) Fujii, T.; Rondelez, Y. Predator - Prey molecular ecosystems. *ACS Nano* **2013**, *7*, 27–34.

- 515 (34) Gines, G.; Zadorin, A. S.; Galas, J.-C.; Fujii, T.; Estevez-Torres, A.; Rondelez, Y.
516 Microscopic agents programmed by DNA circuits. *Nature Nanotechnology* **2017**, *12*,
517 351–359.
- 518 (35) Freeman, R.; Stephanopoulos, N.; Álvarez, Z.; Lewis, J. A.; Sur, S.; Serrano, C. M.;
519 Boekhoven, J.; Lee, S. S.; Stupp, S. I. Instructing cells with programmable peptide
520 DNA hybrids. *Nature Communications* **2017**, *8*, 15982.
- 521 (36) Boshtam, M.; Asgary, S.; Kouhpayeh, S.; Shariati, L.; Khanahmad, H. Aptamers
522 Against Pro- and Anti-Inflammatory Cytokines: A Review. *Inflammation* **2017**, *40*,
523 340–349.
- 524 (37) Shenshin, V. A.; Lescanne, C.; Gines, G.; Rondelez, Y. A small-molecule chemical
525 interface for molecular programs. *Nucleic Acids Research* **2021**, *49*, 7765–7774.
- 526 (38) Zadeh, J. N.; Steenberg, C. D.; Bois, J. S.; Wolfe, B. R.; Pierce, M. B.; Khan, A. R.;
527 Dirks, R. M.; Pierce, N. A. NUPACK: Analysis and design of nucleic acid systems.
528 *Journal of Computational Chemistry* **2011**, *32*, 170–173.
- 529 (39) Wakamatsu, T.; Kitamura, Y.; Kotera, Y.; Nakagawa, N.; Kuramitsu, S.; Masui, R.
530 Structure of RecJ exonuclease defines its specificity for single-stranded DNA. *J Biol*
531 *Chem* **2010**, *285*, 9762–9.